JOURNAL OF MATERIALS SCIENCE 27 (1992) 2734–2738

Sintering aids for ceria–zirconia alloys

S. MASCHIO, O. SBAIZERO, S. MERIANI
Istituto di Chimica Applicata e Industriale, Universitá di Trieste, 34100 Trieste, Italy
E. BISCHOFF,
Max Planck Institut fur Metallforschung, Institut fur Werkstoffwissenschaften, Stuttgart, Germany

Copper and manganese additives for pressureless sintering of Ce–TZP have been studied, the former because its atomic radius is close to that of Ce^{4+}, the latter because its atomic radius is close to that of Zr^{4+}. The temperature at which shrinkage begins did not decrease when using CuO or MnO_2, but at a given temperature, the sintering rate was higher. CuO and MnO_2 were also very effective in improving both the tetragonal phase content retained at room temperature and the mechanical properties (hardness, bending strength and toughness).

1. Introduction

The ceria–zirconia system is being developed as an alternative to the yttria–zirconia system because of its better performance in a moist environment [1], good mechanical properties [2], lower price and wider range of solubility. Furthermore, it is interesting because of the presence of two tetragonal phases [3], one of which, in fact, might give an additional improvement to the mechanical properties through the crack deflection mechanism. Unfortunately, solid solutions with CeO_2 as fluorite-type stabilizer, showed a limited sinterability and even expensive methods such as hot- or hot-isostatic pressing were not suitable because cerium is reduced from Ce^{4+} to Ce^{3+} during the process and ZrO_2 undergoes the tetragonal (t) to monoclinic (m) transformation [4].

The aim of this work was to investigate the effectiveness of additives (CuO, MnO_2) for the pressureless sintering of Ce–TZP, taking into account that in order to obtain appropriate mechanical properties, the material must contain almost 100% tetragonal phase and be as close as possible to the theoretical density to avoid defects which may provide easy crack initiation. It is already known that some transition metals oxides affect the densification behaviour of zirconia-based materials and among them we selected copper and manganese; the former because its atomic radius is close to that of Ce^{4+}, the latter because its atomic radius is close to that of Zr^{4+} [5].

After some preliminary tests, we found that for both oxides a 0.3 mol% was the most effective addition.

2. Experimental procedure

$CeCl_3{\cdot}nH_2O$ (Ce(III)-cloride heptahydrate 99%), 0.05 M solution was used as starting material. Cerium carbonate was precipitated by adding urea and then boiling the solution for 3 h. The white salt was washed with H_2O, dried and calcined at 750° C. The resulting oxide was sieved through a 75 μm screen and mixed with ZrO_2 (m-ZrO_2 99.9%, TZO) in order to give a 12 mol% CeO_2-TZP. The powders were mixed and homogenized by the flo-deflocculation route [6] using HCl (pH 2) and NH_3 solution (pH 8). After flocculation the clear supernatant was removed and the wet powder was washed several times with distilled water to remove cloride ions, then dried.

In order to study the influence of additives on the sinterability, the dried Ce–TZP powder was divided in three batches: (1) as-prepared powder, labelled Ce–TZP; (2) as-prepared powder + CuO (0.3 mol%), labelled Ce–TZP + Cu; (3) as-prepared powder + MnO_2 (0.3 mol%), labelled Ce–TZP + Mn. Oxide powders (CuO and MnO_2) were added and ball milled in plastic jars with zirconia balls for 30 h with an organic binder and 3 h with an organic lubricant, dried, granulated through 75 μm screen, uniaxially pressed at 200 MPa to form pellets of 10 mm diameter.

The green compacts, about 45 % theoretical density, were sintered in air at 1450 and 1530° C, respectively, for various periods of time. Dilatometric tests were performed with a Netzsch dilatometer in air and oxygen, with a heating rate of 10 K min^{-1}.

The following measurements were made on the sintered bodies. Archimede's method to measure densities; X-ray diffraction, CuK_α (nickel-filtered), for phase identification; and the Garvie and Nicholson method [7] to assess the tetragonal to monoclinic ratio; SEM pictures and the intercept method to estimate the average grain size; SEM and TEM analysis to examine the microstructure under the additives' influence. Modulus of rupture was measured with a four-point bend jig (30 mm outer, 10 mm inner span) and a crosshead speed of 0.1 mm min^{-1}, on 40 mm × 7 mm × 3 mm bars. Hardness was measured by Vicker's indentation with loads ranging from 90 to 200 N; lower loads were necessary in those materials where the monoclinic phase was present. The fracture toughness was assessed by indentation strength in bending (ISB) technique using a Vicker's indentor, with a 200 N load, then breaking the specimen by the four-point bending test.

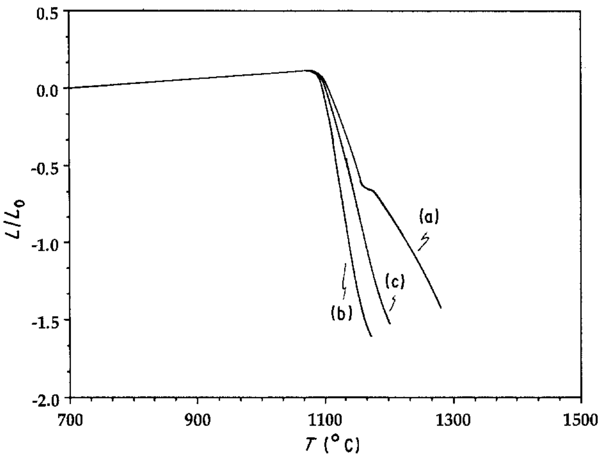

Figure 1 Dilatometric curves for the different starting powders. (a) Ce–TZP, (b) Ce–TZP + Cu, (c) Ce–TZP + Mn.

3. Results and discussion

The sintering plots of the three samples behaved in the same way as shown in Fig. 1. The thermal expansion of the pressed samples was the same, moreover the onset shrinkage temperature (1120° C) remained unchanged but the powders behaved differently after the initial shrinkage stage; pure Ce–TZP displayed a two-step densification (at 1220° C), whereas powders with either CuO or MnO_2 densified in a single step. SEM analysis on Ce–TZP samples fired at 1220° C revealed that the particles were already partially sintered, leaving large intergranular voids which, being difficult to eliminate, hindered further densification. With extended heating it was possible to increase shrinkage but, at the same time, anomalous grain growth took place.

Densification curves for the pressureless sintered samples in air at 1450 and 1530° C are shown in Fig. 2 (separate samples were used to obtain the individual data points). Ce–TZP compacts required a very high temperature and long firing cycles to reach high densities; however, these latter (final density) may appear still low if compared with those usually obtained with some commercial Ce–TZP powders. It should be pointed out that our powders were prepared with a

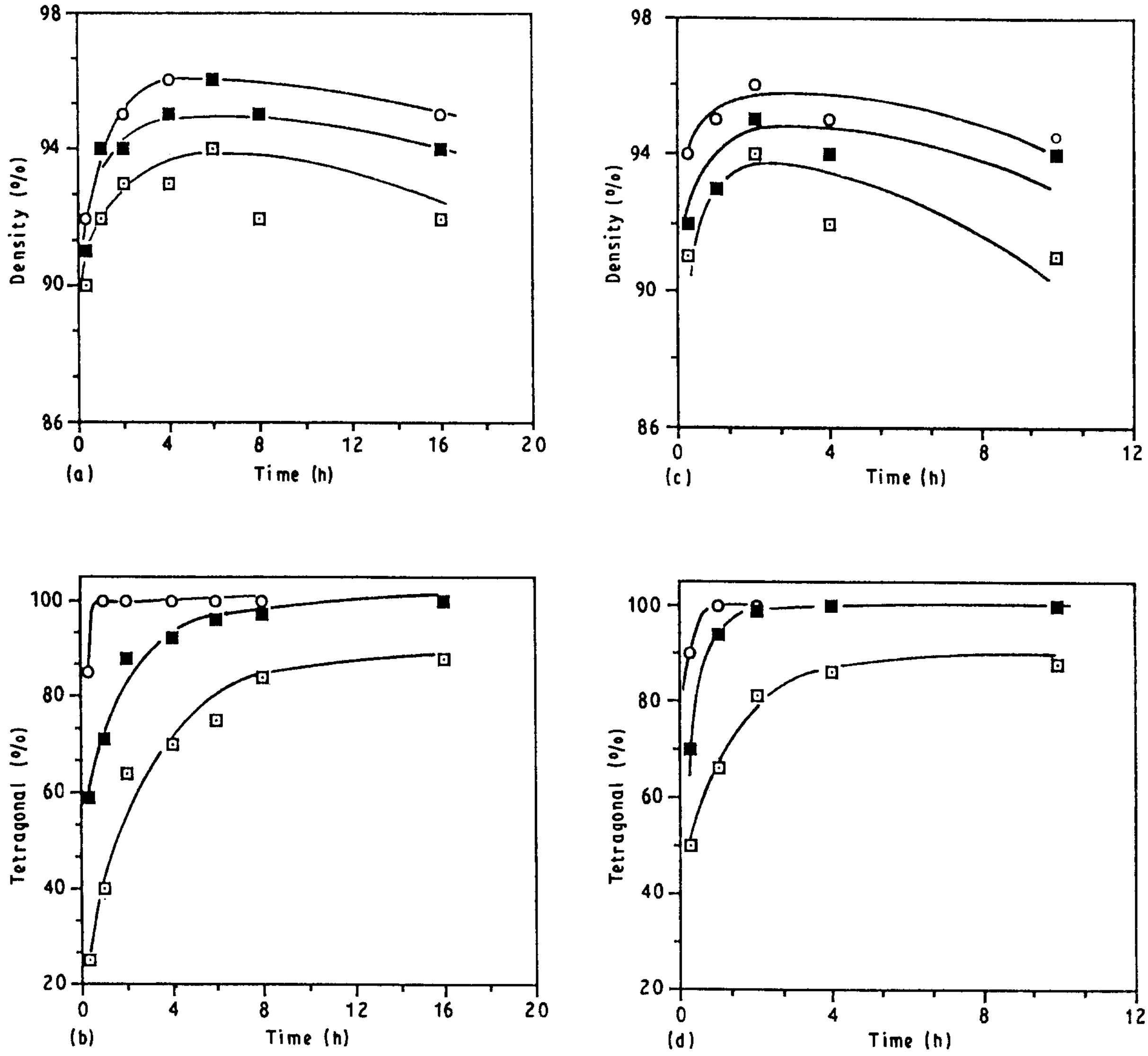

Figure 2 Density and amount of tetragonal phase of sintered samples versus sintering time for: (a, b) 1450°C, (c, d) 1530°. (⊡) Ce–TZP, (○) Ce–TZP + Cu, (■) Ce–TZP + Mn.

non-conventional method, and that green compacts were unaxially pressed; therefore, as a bench mark, only a compact with low final density could be obtained. On the other hand, both CuO and MnO_2 additions enhanced densification as well as the amount of tetragonal phase retained at room temperature. CuO had the strongest effect, whereas MnO_2 was slightly less effective, but both remarkably changed the amount of tetragonal phase, i.e. after 2 h, at 1450° C a fully tetragonal body could be obtained.

From Fig. 2 it is possible to see that samples sintered either at 1450 or 1530° C exhibited maximum density after 4 and 2 h, respectively. After this time, the amount of tetragonal phase increased (in the case of undoped material) but density decreased slightly.

All these samples were sintered within a temperature range where the Ce^{4+}/Ce^{3+} redox equilibrium becomes appreciable. The presence of Ce^{3+} species is accompanied by oxygen evolution and vacancies formation but also by the destabilization of the tetragonal phase which, on becoming monoclinic, may give rise to microcracking and density decrease. The phenomenon of Ce^{3+} reduction and retention occurs mostly within the body, away from the sample surface. This latter, on cooling, promptly reacts with the atmospheric oxygen to restore the Ce^{4+} valence and the tetragonal-phase concentration.

Fig. 3 shows the grain-growth kinetics of Ce–TZP, for a constant temperature, with and without dopants. It can be seen that samples without dopants had a grain size about two-fold larger than those doped. For example, in this log–log plot, the slope for the Ce–TZP is 0.54, whereas for the copper-doped samples it is 0.27 and for the manganese-doped samples it is 0.20. The grain-growth kinetics can be expressed as

$$G^n(t) - G^n(0) = kt \qquad (1)$$

where $G(t)$ is the grain size after the sintering time, t; $G(0)$ is the grain size extrapolated at time $t = 0$; k is a proportionality constant and n is the growth exponent. For Ce–TZP, $n \approx 1.9$ whereas copper and manganese dopants increased the growth exponent n, to ≈ 3.5 and ≈ 4.5, respectively.

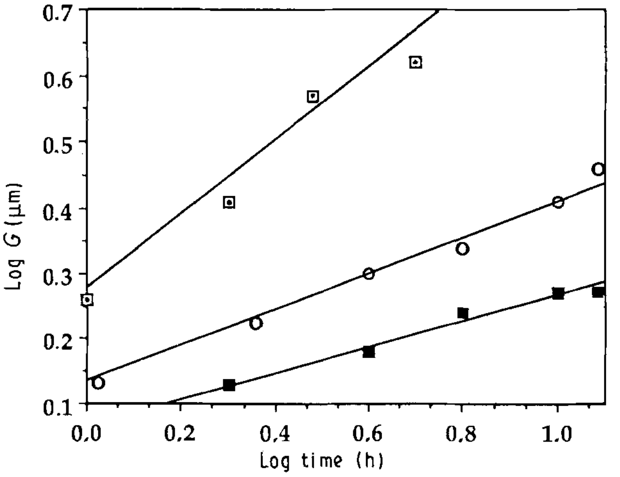

Figure 3 Grain-growth kinetics of Ce–TZP samples showed by a log–log plot of grain size versus sintering time. (⊡) Ce–TZP, (■) Ce–TZP + Mn, (○) Ce–TZP + Cu.

Fig. 4 shows the microstructure of samples sintered for 4 h at 1530° C. The resulting microstructure was made of large homogeneous grains about 4–5 μm in the pure Ce–TZP, 2 μm when CuO was used, and 1.4 μm when MnO_2 was used.

TEM analysis, Fig. 5, revealed the presence of a liquid phase at the triple-point grain boundaries (pockets) only when CuO was used, due to the fact that the eutectic melting temperature of $CuO/Cu_2O–ZrO_2$

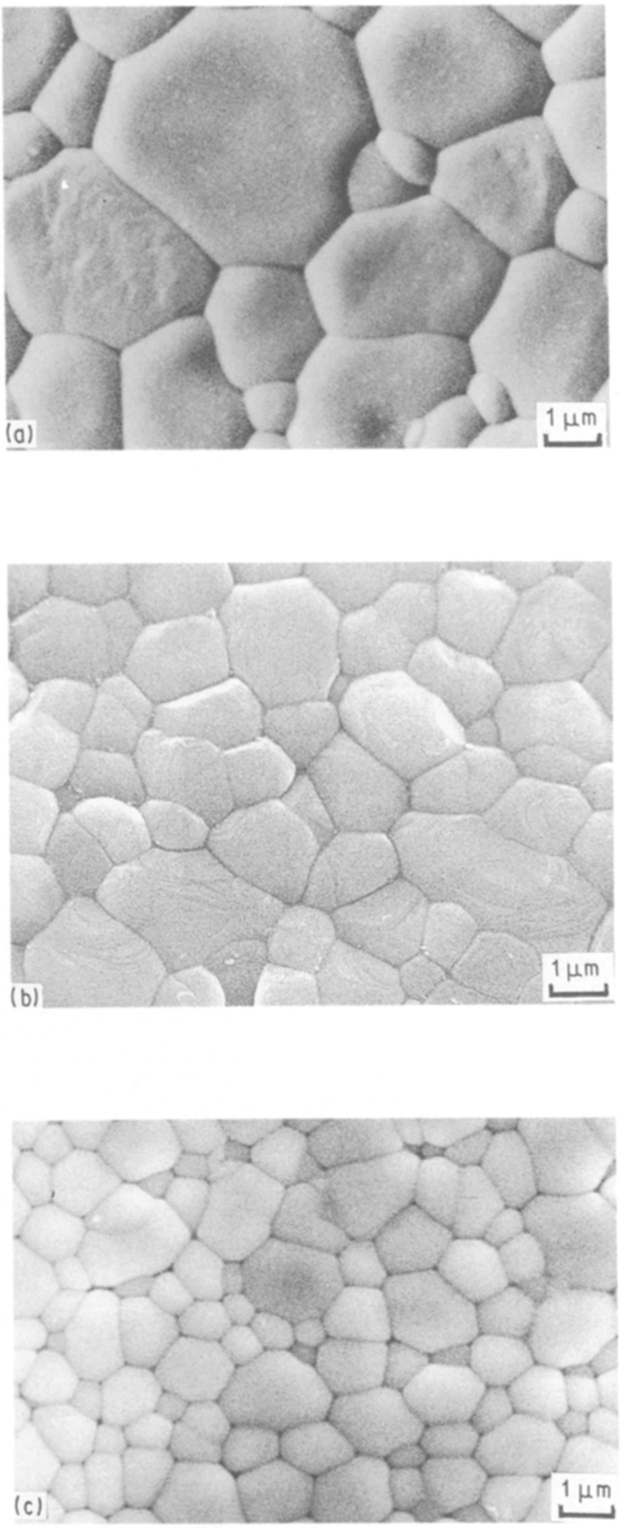

Figure 4 Scanning electron micrographs of the Ce–TZP materials sintered at 1530° C for 4 h: (a) Ce–TZP, (b) Ce–TZP + Cu, (c) Ce–TZP + Mn.

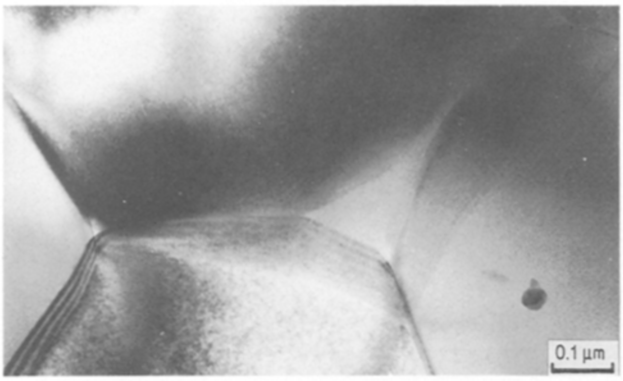

Figure 5 Transmission electron micrograph of Ce–TZP + Cu material showing a glassy phase pocket at the triple point.

is 1130° C in air. We have been unable to identify any manganese-rich layer; probably the glassy phase could not be detected by our technique. These experimental results showed that under the same sintering conditions, small amounts of CuO could improve the sintering of Ce–TZP more effectively that MnO_2, but the latter was stronger in depleting the rate of grain growth. It is hard to explain the reasons for these different effects. The influence of dopants on densification should be discussed on the basis of the defect-forming ability of the ions available after the first sintering stage, which is common to both the pure and doped materials. Both CuO and MnO_2 undergo a high temperature reduction forming Cu_2O and $MnO_2 \cdot Mn_2O_3$, respectively. New ionic species, such as Cu^+ and Mn^{2+} become available at 1200° C and these can possibly interact with the sinter-reactive ceria and zirconia particles which, both being tetravalent, do not introduce oxygen vacancies into the crystal lattice of their solid solutions.

It has been assumed that in stabilized zirconias the defect structure is fixed by the amount of the aliovalent stabilizers such as Ca^{2+} and Y^{3+}. Any other dopant present in a small quantity cannot possibly modify either the defects' number and structure of the host matrix, nor the lattice diffusion coefficient of the controlling species. This is not the case in ceria–zirconia materials where the stabilizer (CeO_2) has the same stoichiometry as the host (ZrO_2) matrix, at least up to a certain temperature. In this solid solution the dopants become relevant in introducing lattice defects and enhancing cation diffusion through oxygen vacancy formation; furthermore when Ce^{4+} is reduced to Ce^{3+} to balance its lower oxidation state, oxygen vacancies are introduced.

From this point of view, two Cu^+ ions introduce three double-charged oxygen vacancies, whreas one Mn^{2+} or two Mn^{3+} ions form one vacancy only. Both can modify the lattice defect structure and the diffusion coefficient of the rate-controlling species, namely cerium and zirconium cations [8, 9]. These differences might depend upon the different dopant's charges as well as ionic radii; in fact, in ceramics, the interaction between solutes and grain boundaries originates from (1) the electrostatic force between the charged ions and the electrical double layers in the grain boundary region, and (2) the stress due to the ionic size misfit between the solute and the matrix ions. The theory most often used to explain the effect of a solute on grain-boundary motion is the Cahn solute drag model [10], which is based on solute segregation at (or away from) the grain boundaries. In this theory the drag force on grain-boundary motion is due to an interaction energy between grain boundaries and solutes. When grain boundaries migrate, solutes tend to follow them; because solutes are usually less mobile than grain boundaries, the grain-boundary velocity is decreased by the solute drag force; Cu^+ is larger than either Mn^{3+} or Mn^{2+} and, therefore, one would expect Cu^+ to be a stronger segregant and a more effective grain-growth inhibitor. Nevertheless, this simple solute segregation argument is deficient. During zirconia sintering, densification is assumed to be achieved by lattice diffusion, $\mathscr{D}_l$, and coarsening by surface diffusion mechanism $\mathscr{D}_s$. From this standpoint, it can be concluded that both CuO and MnO_2 affect the ratio, $\mathscr{D}_l/\mathscr{D}_s$, but with different effectiveness. The reason why CuO improves the sintering rate more than MnO_2 does seem to rely more upon the defect-forming ability of the Cu^+ species being more effective than Mn^{2+}.

Cu^+ and Ce^{4+} ionic radii are in addition, very close, both contributing by the same extent to the zirconia lattice distortion. On the other hand, as the Mn^{2+} and Zr^{4+} ionic radii are quite similar; neither distortion nor enhanced stabilization of the tetragonal form is expected on its addition. In fact, this evidence is reflected by the mechanical properties and the materials microstructure. The mechanical properties obtained with samples sintered at 1530° C for 4 h are reported in Table I. The addition of either copper or manganese increased hardness because of the smaller grain size. SEM investigations showed that in doped samples at room temperature, intergranular fracture has been more often found, whereas in the pure Ce–TZP, transgranular fracture was predominant. Although mechanical properties were enhanced and quite good for both doped materials, manganese appeared to be more effective than copper in raising toughness and bending strength. The small difference in the average grain size, between the two doped materials, could be responsible for the relatively different mechanical properties.

TEM analysis, Fig. 6, revealed that twins were often present in the Ce–TZP + Mn microstructure, whereas they have seldom been found in the Ce–TZP + Cu materials. This suggests that the transformation toughening mechanism was more likely to occur in the

TABLE I Mechanical properties obtained after sintering at 1530° C for 4 h

Materials	Tetragonal (%)	σ (MPa)	H_v (GPa)	K_{Ic} (MPa/m$^{1/2}$)
Ce–TZP	84	150	6	8
Ce–TZP + CuO	100	350	8	11
Ce–TZP + MnO_2	100	450	8	14

Figure 6 Photomicrograph Ce–TZP + Mn showing twins formed during the TEM analysis.

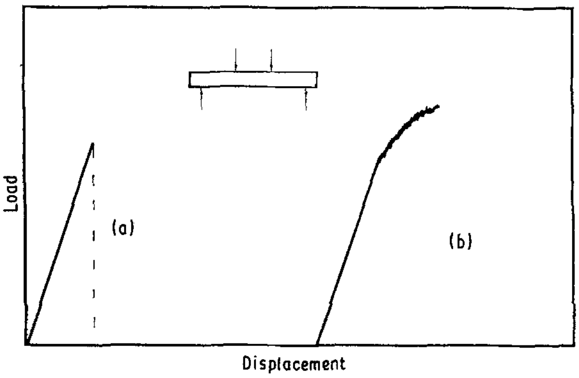

Figure 7 Load–displacement plots in four-point bending for: (a) Ce–TZP + Cu, (b) Ce–TZP + Mn sintered for 4 h at 1530° C.

manganese-doped material. Probably there is an overstabilization of the tetragonal phase with copper additions, because of the introduction of Cu^+ ions, very close in size to the Ce^{4+} species, increasing the amount of the non-transformable fully stabilized Ce–TZP. On the contrary, Mn^{2+} ions may increase the amount of the transformable (t) Ce–TZP phase, contributing to enhance the material's toughness.

The higher toughness of the manganese-doped material was also accompanied by an increasingly pronounced deviation of the macroscopic stress–strain curve from the linear relationship which was found for copper-doped material, Fig. 7 [11]. The stable deformation of the Ce–TZP + Mn sample is interrupted by repeated load drops that are due to the transformation bands developed on the tensile surface of flexure bars [12, 13].

4. Conclusions

CuO and MnO_2 have shown to be good candidates as additives for the pressureless sintering of ceria-stabilized zirconia.

High density, small grain size, as well as almost fully tetragonal material could be achieved using short sintering times at a reasonable temperature. The temperature at which the shrinkage began did not decrease using MnO_2 or CuO, but at the same temperature the sintering rate was higher. MnO_2 and CuO were also very effective in improving mechanical properties (hardness, bending strength and toughness); manganese giving the higher toughness with a non-linear stress–strain curve.

Acknowledgements

This work was performed with financial support from the Italian National Research Council (PNF Special Materials for Advanced Technologies) and the Ministry of Public Education.

References

1. R. L. K. MATSUMOTO, *J. Amer. Ceram. Soc.* **71** (1978) C 128.
2. K. TSUKUMA and M. SHIMADA, *J. Mater. Sci.* **20** (1985) 1178.
3. S. MERIANI, *Mater. Sci. Engng* **71** (1985) 369.
4. T. SATO, T. ENDO and M. SHIMADA, in "Zirconia.'88: Advances in Zirconia Science and Technology", edited by S. Meriani and C. Palmonari, (Elsevier Applied Science, London, 1989) pp. 293–300.
5. L. PAULING, "The nature of the Chemical Bond" (Cornell University Press, Ithaca, NY, 1940).
6. F. F. LANGE and M. M. HIRLINGER, *J. Amer. Ceram. Soc.* **67** (1984) 164.
7. R. C. GARVIE and P. S. NICHOLSON, *J. Amer. Ceram. Soc.* **55** (1972) 303.
8. R. J. BROOK, in "Science and technology of zirconia", edited by A. H. Heuer and L. W. Hobbs (American Ceramic Society, Columbus, OH, 1981) pp. 272.
9. S. WU and R. J. BROOK, *Trans. J. Ceram. Soc.* **82** (1983) 200.
10. H. M. CAHN, *Acta Metall.* **10** (1962) 789.
11. R. H. J. HANNINK and M. SWAIN, *J. Amer. Ceram. Soc.* **72** (1989) 90.
12. P. E. REYES-MOREL, J. S. CHERNG and I. CHEN, *ibid.* **71** (1989) 648.
13. C. SCHMID, H. SCHUBERT, S. MERIANI, "The role of alumina in zirconia-ceria composite alloys", "Euro Ceramics" Vol. 1, edited by G. de With, R. A. Terpstra and R. Metselaar (Elsevier Applied Science, London, NY, 1989) pp. 1547–53.

Received 23 January
and accepted 7 June 1991